2-1-2006

# Structures and relative stability of medium-sized silicon clusters. IV. Motif based low-lying clusters $Si_{21}$–$Si_{30}$

Soohaeng Yoo
*University of Nebraska-Lincoln*

Xiao Cheng Zeng
*University of Nebraska-Lincoln*, xzeng1@unl.edu

# Structures and relative stability of medium-sized silicon clusters. IV. Motif-based low-lying clusters $Si_{21}$–$Si_{30}$

Soohaeng Yoo and X. C. Zeng[a)]
*Department of Chemistry and Center for Materials Research and Analysis, University of Nebraska-Lincoln, Lincoln, Nebraska 68588*

(Received 24 October 2005; accepted 14 December 2005; published online 1 February 2006)

Structures and relative stability of four families of low-lying silicon clusters in the size range of $Si_n$($n$=21–30) are studied, wherein two families of the clusters show prolate structures while the third one shows near-spherical structures. The prolate clusters in the first family can be assembled by connecting two small-sized magic clusters $Si_n$ ($n$=6, 7, 9, or 10) via a *fused-puckered-hexagonal-ring* $Si_9$ unit (a fragment of bulk diamond silicon), while those in the second family can be constructed on the basis of a structural motif consisting of a *puckered-hexagonal-ring* $Si_6$ unit (also a fragment of bulk diamond silicon) and a small-sized magic cluster $Si_n$ ($n$=6, 7, 9, or 10). For $Si_{21}$–$Si_{29}$, the predicted lowest-energy clusters (except $Si_{27}$) exhibit prolate structures. For clusters larger than $Si_{25}$, the third family of near-spherical clusters becomes energetically competitive. These near-spherical clusters all exhibit endohedral cagedlike structures, and the cages are mostly homologue to the carbon-fullerene cages which consist of pentagons and hexagons exclusively. In addition, for $Si_{26}$–$Si_{30}$, we construct a new (fourth) family of low-lying clusters which have "Y-shaped" three-arm structures, where each arm is a small-sized magic cluster ($Si_6$, $Si_7$, or $Si_{10}$). Density-functional calculation with the B3LYP functional shows that this new family of clusters is also energetically competitive, compared to the two prolate and one near-spherical low-lying families. © *2006 American Institute of Physics*.
[DOI: 10.1063/1.2165181]

## I. INTRODUCTION

Over the past two decades, theoretical investigation of the structures and relative stability of medium-sized silicon clusters $Si_n$ ($n \geqslant 11$) has been an active area of research.[1–42] Major efforts have been undertaken towards finding the global-minimum structures for $n \geqslant 11$. For example, Jackson and co-workers reported systematic searches for the global minima of silicon cation and neutral clusters in the medium size range of $19 \leqslant n \leqslant 28$, using either the single-parent evolution algorithm or the big-bang algorithm coupled with density-functional tight-binding (DFTB) method.[20,41,42] Recently, the size range of $25 \leqslant n \leqslant 29$ has received increasing attention[32–36,39–42] largely because earlier experiments[43–48] have revealed a structural transition from prolate to near-spherical geometry at $n \sim 27 \pm 2$, for both cation and anion silicon clusters. A more recent experimental/theoretical photoelectron-spectroscopy study[49] also confirmed the structural transition occurring at $n=27$ for anion clusters. To date, the true global minima for many clusters in the size range of $13 \leqslant n \leqslant 29$ are still debatable,[36–42] due in part to the subtle sensitivity of predicted global minima on the density functional selected (e.g., PBE or B3LYP functional), or the level of molecular-orbital theory selected [e.g., MP2 or CCSD(T)] in the *ab initio* calculations.[26] Moreover, as the size of the cluster increases, finding the true global minima becomes increasingly a challenge because of the much increased number of low-lying isomers. Nevertheless, previous tight-binding (TB) and DFTB-based global-minimum searches have shed much light on some generic structural features of low-lying clusters in the size range of $13 \leqslant n \leqslant 30$. For example, most low-lying clusters in the size range of $13 \leqslant n \leqslant 22$ likely belong to two families, one containing the tricapped-trigonal-prism (TTP) $Si_9$ motif[16,39] while another containing the six/six $Si_6/Si_6$ motif (a *puckered-hexagonal-ring* $Si_6$ plus *tetragonal bipyramid* $Si_6$).[20,36,37] For $27 \leqslant n \leqslant 40$, it was found that carbon fullerenes can serve as generic cage motifs[8,11,24] to form "stuffed fullerenelike" low-lying clusters.[35] As discussed in Ref. 37 (Paper III of this series), identification of these *generic* structural features not only can dramatically reduce computation cost for *ab initio* calculation of the potential-energy surface but also can provide additional physical insight into growth patterns of medium-to-large-sized low-lying clusters.

In this article, geometric structures and relative stability of four families of low-lying clusters in the size range of $21 \leqslant n \leqslant 30$ are further examined. Among them, two families that exhibit prolate structures can be constructed based on various generic structural motifs. The third family, which has near-spherical structures, can be obtained via constrained (biased) search based on the fullerene cage motifs. A new (fourth) family is reported to have "Y-shaped three-arm" structures. Specifically, those prolate clusters in the first family can be assembled by connecting two small-sized magic clusters $Si_n$ ($n$=6, 7, 9, or 10) via a fused-puckered-hexagonal-ring $Si_9$ unit (a fragment of bulk diamond silicon), and those in the second family can be constructed on basis of

a)Electronic mail: xczeng@phase2.unl.edu

 

a structural motif consisting of a puckered-hexagonal-ring $Si_6$ (also a fragment of bulk diamond silicon) and a small-sized magic clusters $Si_n$ ($n$=6, 7, 9, and 10). Note that evidences of these "small-cluster-assembled" medium-sized clusters have also been observed in the previous cluster-dissociation experiments. For example, Smalley and co-workers[50,51] reported photodissociation studies of silicon clusters containing up to 60 atoms and they found that medium-sized clusters with less than 30 atoms dissociate mainly by loss of the small-sized magic-number clusters $Si_6$, $Si_7$, and $Si_{10}$. Jarrold and Bower[52] conducted collision-induced dissociation experiment to monitor dissociation of silicon cluster cations containing up to 26 atoms and they found that clusters with 19–26 atoms dissociate mainly by loss of $Si_{10}$ unit. Indeed, these early experiments support the notion that medium-sized low-lying clusters can be built based on small-sized magic clusters $Si_6$, $Si_7$, $Si_9$, and $Si_{10}$.

## II. COMPUTATIONAL DETAILS

Geometric optimization and total-energy calculations for all clusters were performed by using methods of density-functional theory (DFT) implemented in two software packages: (1) the plane-wave-pseudopotential density-functional theory (PWP-DFT) with generalized-gradient approximation (GGA) [Two functionals were selected, the Becke exchange and Lee-Yang-Parr correlation (BLYP) functional[53] and the Perdew-Burke-Ernzerhof (PBE) functional,[54] both implemented in the CPMD program.[55]] and (2) the all-electron DFT method at the B3LYP/6-31G ($d$) level, compiled in the GAUSSIAN 03 software package.[56] The reason to use three different functionals is to examine possible functional dependence of the predicted lowest-energy isomers, which was shown to occur for smaller-sized clusters in Paper III.[37] In our previous studies of smaller-sized clusters $Si_n$($n$=7–20) (Refs. 25 and 26) (Papers I and II in this series) we used *ab initio* molecular-orbital methods at the MP2/6-31G($d$) level of theory for geometry optimization and the coupled-cluster level of theory for total-energy calculation. However, for the size range considered here, geometry optimization at the MP2/6-31G($d$) level and particularly total-energy calculation at the coupled-cluster level of theory will be computationally very demanding. We therefore only report results based on PWP-DFT and B3LYP/6-31G($d$) calculations. Note that in the PWP-DFT calculations, we used a cutoff energy 30 Ry for plane-wave expansion and a supercell size with the dimension of 25 Å.

## III. RESULTS

### A. Family I: Prolate clusters for 21≤$n$≤29

Prolate clusters in family I can be constructed by connecting two small-sized magic clusters $Si_n$ ($n$=6, 7, 9 or 10) through a *fused-puckered-hexagonal-ring* $Si_9$ unit. The latter can be viewed as a fragment of bulk diamond silicon [see Fig. 1(a)] and it serves as a "glue unit" to hold two small-sized magic clusters together. In Fig. 1(b) we display four small-sized magic clusters as the "parts" for assembling the low-lying prolate clusters, namely, $Si_6$ (distorted octahedron), $Si_7$ (pentagonal bipyramid), $Si_9$ (TTP), and $Si_{10}$ (tetracapped trigonal prism). As shown in Paper I (Fig. 5 in Ref. 25), the incremental binding energy of $Si_8$ is notably smaller than $Si_6$, $Si_7$, $Si_9$, and $Si_{10}$. Therefore, the global-minimum structure of $Si_8$ (distorted-bicapped octahedron) is not a favored part for the assembly. Likewise, the global minimum of $Si_{11}$(pentacapped trigonal prism) is not a favored part neither.

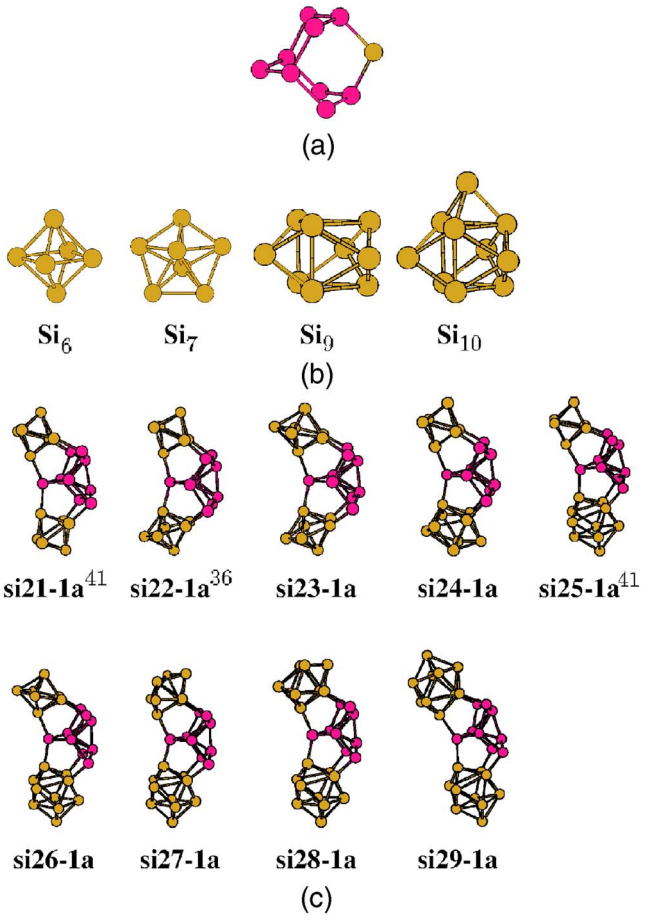


FIG. 1. (Color online) (a) A nine-atom unit—the *fused-puckered-hexagonal-ring* $Si_9$—highlighted in pink color. This unit can be viewed as bulk fragment of the cubic diamond silicon—"adamantane" $Si_{10}$. (b) Small-sized magic clusters as "parts" for assembling low-lying prolate clusters in families I, II, and IV. These parts include $Si_6$ (distorted octahedron), $Si_7$ (pentagonal bipyramid), $Si_9$ [tricapped trigonal prism (TTP)], and $Si_{10}$ (tetracapped trigonal prism). (c) Geometries of clusters with lowest energy in family I. The "glue part," namely, the fused-puckered-hexagonal-ring $Si_9$ is highlighted in pink color.

In Fig. 1(c), we display prolate clusters ($Si_{21}$–$Si_{29}$) in family I where the notation **1a** refers to the isomer that has the lowest energy in family I. For $Si_{21}$–$Si_{24}$, $Si_{26}$, $Si_{28}$, and $Si_{29}$ the structural assembly is unique. However, for $Si_{25}$ and $Si_{27}$, there are two possible structural assemblies. $Si_{25}$ can be viewed either as an assembly of $Si_6$+$Si_9$ (glue unit) +$Si_{10}$ or an assembly of $Si_7$+$Si_9$ (glue unit) +$Si_9$. Since the incremental binding energy of $Si_6$ and $Si_{10}$ is higher than $Si_7$ and $Si_9$, the assembly of $Si_6$+$Si_9$ (glue unit) +$Si_{10}$ (si25-1a) has a lower energy than the assembly of $Si_7$+$Si_9$ (glue unit) +$Si_9$. For $Si_{27}$, also, there are two competing assemblies, $Si_8$+$Si_9$ (glue unit) +$Si_{10}$ and $Si_9$+$Si_9$ (glue unit) +$Si_9$. Note that since the structure of the $Si_8$ portion is unknown *a priori*, we performed a constrained (or biased) basin-hopping search

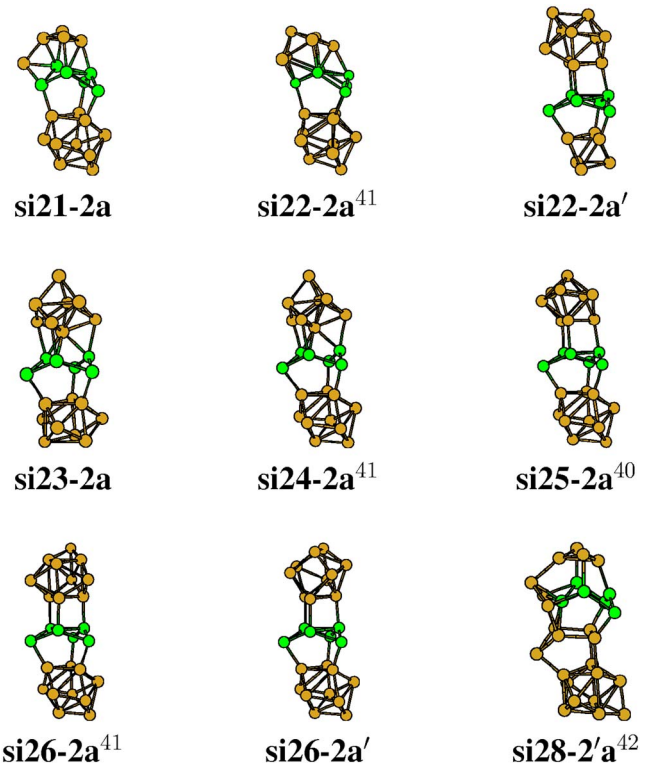


FIG. 2. (Color online) Geometries of clusters with lowest energy in family II. The glue part, namely, the *six-fold-puckered-ring* $Si_6$ appeared in the six/six, six/nine, and six/ten structural motifs is highlighted in green color.

combined with DFT optimization[36,37] to obtain the final $Si_8$ structure when attached to the $Si_9$ (glue unit) $+Si_{10}$ portion of the cluster. Total-energy calculations show that the assembly of $Si_8+Si_9$ (glue unit) $+Si_{10}$ (si27-1a) is slightly lower in energy (~0.14 eV) than the assembly of $Si_9+Si_9$ (glue unit) $+Si_9$. Finally, we note that si30-1a may be viewed as an assembly of $Si_{11}+Si_9$ (glue unit) $+Si_{10}$. Since the $Si_{11}$ cluster is not favored energetically, si30-1a is not displayed in Fig. 1(c).

### B. Family II: Prolate clusters for $21 \leqslant n \leqslant 26$

Prolate clusters in family II can be constructed on the basis of the structural motif consisting of a puckered-hexagonal-ring $Si_6$ (also a fragment of bulk diamond silicon) and a small-sized magic clusters $Si_n$ ($n=6$, 7, 9, or 10). The resulting structural motifs can be named as the *six/six, six/seven, six/nine*, or *six/ten* motif, repectively.[36,37] The structure of the remaining portion of the cluster has to be determined via constrained (or biased) basin-hopping search coupled with DFT geometry optimization.[36,37] Previously, we reported that clusters based on the six/six motif can be energetically competitive starting from $n=16$ and up to $n=22$.[36] For $n \geqslant 24$, our constrained search indicates that the six/ten motif gives rise to the lowest-energy isomers in family II, consistent with the previous global search of Jackson *et al.*[41] In Fig. 2 we display the lowest-energy isomers for cluster in the size range of $21 \leqslant n \leqslant 26$. Here the notation **2a** denotes the lowest-energy isomer in family II (calculated using the PBE functional) while **2a′** denotes the lowest-energy isomer (calculated using BLYP or B3LYP functional). As shown in Fig. 2, there are two isomers of $Si_{22}$ and $Si_{26}$ which compete for the lowest-energy isomer. This is mainly due to the functional dependence, which has been discussed more extensively in Paper III.[37] We found that if the PBE functional is selected, the constrained search indicates that si22-2a and si26-2a are lower in energy than si22−2a′ and si26-2a′, respectively whereas if the BLYP (or B3LYP) functional is selected, the search indicates otherwise. For other clusters, calculations with both PBE and BLYP functionals give consistent prediction to the lowest-energy isomer in family II.

In Fig. 2, we also display a prolate isomer of $Si_{28}$. Strictly speaking, this isomer does not belong to family II since the puckered-hexagonal-ring $Si_6$ unit is not directly attached to the $Si_{10}$ magic cluster. This $Si_{28}$ isomer was obtained by Jackson *et al.*[42] through an unbiased search and is the leading candidate for the global minimum of $Si_{28}$. We therefore refer it as si28-2′a because it shows certain structural similarity to clusters in family II.

### C. Family III: Near-spherical cagedlike clusters for $25 \leqslant n \leqslant 30$

Low-lying clusters with near-spherical structures have been recently reported by Jackson *et al.* (up to $n=28$) (Ref. 41 and 42 and by us (up to $n=45$).[35,49] In Fig. 3, we display those predicted lowest-energy isomers, all have already appeared in the literature. Again, the notation **3a** denotes the lowest-energy isomer in family III (calculated with the PBE functional) while **3a′** denotes the lowest-energy isomer (calculated with the BLYP or B3LYP functional). The functional dependence on the predicted lowest-energy structure is seen for $Si_{25}$, $Si_{28}$, and $Si_{30}$ (see Fig. 3).

As shown previously,[35] the cages of near-spherical clusters are generally homologue to the carbon-fullerene cages which consist of pentagons and hexagons exclusively with even numbers of atoms. In Fig. 3, we highlight the core-filling ("stuffing") atoms by blue color. If these core-filling atoms were removed and the cage atoms were replaced by carbon atoms, we can obtain the corresponding carbon-fullerene cages after structural optimization. Indeed, as shown in Fig. 3, cages of all clusters except two (si25-3a and si27-3a) (Ref. 41) are homologue to the carbon-fullerene cages.

### D. Family IV: Y-shaped three-arm clusters for $26 \leqslant n \leqslant 30$

In light of that magic-cluster-assembled medium-sized clusters can be energetically very favorable in the size range of $Si_{16}$–$Si_{29}$, we attempted to construct a new family of clusters that are composed of a glue unit plus three magic clusters (from $Si_6$–$Si_{10}$). We call this hypothetical (fourth) family of clusters the Y-shaped three-arm clusters (see Fig. 4). The "glue" unit (the red-colored unit in Fig. 4) is very similar to the fused-puckered-hexagonal-ring $Si_9$ unit but with one atom removed. As such, two magic clusters $Si_6$ can be attached to the glue unit symmetrically on two sides, forming two "arms" of the "Y-shaped" clusters. The structure of the third arm can be obtained based on a constrained (or biased) basin-hopping search coupled with DFT optimization.[36] Not

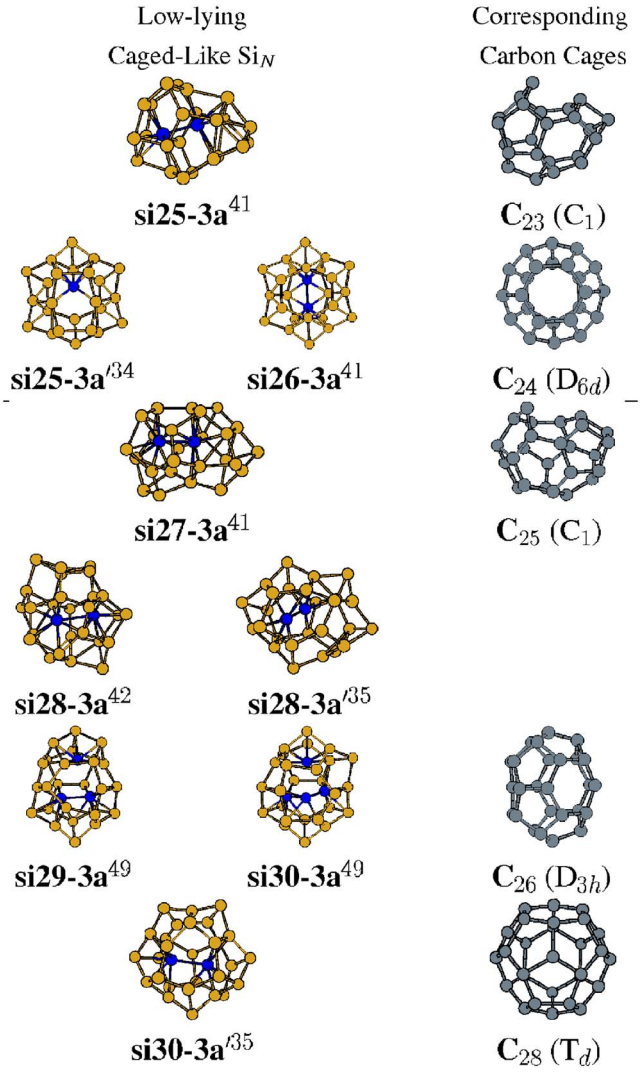


FIG. 3. (Color online) Geometries of clusters with lowest energy in family III. The "stuffing," namely, the endohedral silicon atoms inside the cages are highlighted in blue color. The corresponding homolog carbon cages are displayed in grey color.

surprisingly, the obtained structures of the "third" arm for si26-4a, si27-4a, si29-4a, and si30-4a are those of magic clusters $Si_6$, $Si_7$, $Si_9$ (TTP), and $Si_{10}$, respectively [Fig. 1(b)].

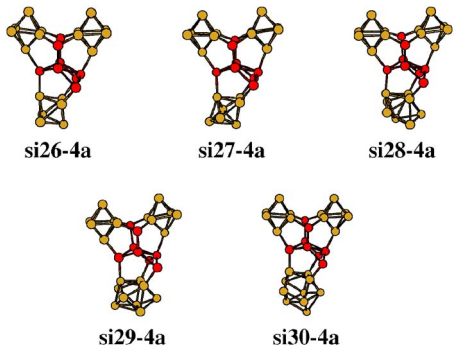


FIG. 4. (Color online) Geometries of clusters with lowest energy in family IV. The "glue" part $Si_8$ is highlighted in red color. The two arms at the top of the Y-shaped three-arm clusters are the magic cluster $Si_6$ [see Fig. 1(b)].

TABLE I. The total-energy differences between the predicted lowest-energy isomer and several other low-lying isomers. The lowest-energy clusters are highlighted using the bold-faced number **0.000**. Those isomers with energy difference less than 0.1 eV from the lowest-energy ones are also highlighted using bold-faced number.

| | CPMD/PBE $\Delta E$ (eV) | CPMD/BLYP $\Delta E$ (eV) | B3LYP/6-31G($d$) $\Delta E$ (eV) |
|---|---|---|---|
| si21-1a | **0.000** | **0.000** | **0.000** |
| si21-2a | 0.253 | 0.452 | 0.445 |
| si22-1a | 0.288 | **0.000** | **0.000** |
| si22-2a | **0.000** | 0.256 | 0.477 |
| si22-2a′ | **0.082** | 0.164 | 0.379 |
| si23-1a | 0.538 | **0.000** | **0.000** |
| si23-2a | **0.000** | **0.005** | 0.175 |
| si24-1a | 0.306 | **0.028** | **0.090** |
| si24-2a | **0.000** | **0.000** | **0.000** |
| si25-1a | **0.000** | **0.000** | **0.000** |
| si25-2a | 0.294 | 0.715 | 0.907 |
| si25-3a | 0.694 | 1.395 | 1.160 |
| si25-3a′ | 0.907 | 0.930 | 0.683 |
| si26-1a | 0.204 | **0.000** | **0.000** |
| si26-2a | **0.000** | 0.307 | 0.501 |
| si26-2a′ | **0.040** | 0.202 | 0.436 |
| si26-3a | **0.012** | 0.465 | 0.367 |
| si26-4a | 0.537 | **0.077** | 0.188 |
| si27-1a | 0.314 | **0.017** | **0.042** |
| si27-3a | **0.000** | 0.357 | 0.136 |
| si27-4a | 0.672 | **0.000** | **0.000** |
| si28-1a | **0.021** | **0.000** | **0.000** |
| si28-2′a | **0.000** | 0.419 | 0.231 |
| si28-3a | **0.072** | 0.747 | 0.374 |
| si28-3a′ | 0.310 | 0.475 | **0.081** |
| si28-4a | 0.891 | 0.570 | 0.551 |
| si29-1a | **0.000** | **0.000** | **0.000** |
| si29-3a | 0.261 | 1.029 | 0.629 |
| si29-4a | 0.939 | 0.783 | 0.862 |
| si30-3a | **0.000** | 1.122 | 0.763 |
| si30-3a′ | 1.168 | 0.868 | 0.484 |
| si30-4a | 0.385 | **0.000** | **0.000** |

## IV. DISCUSSION AND CONCLUSION

Relative stability of low-lying silicon clusters belonging to the four families has been analyzed via their total-energy differences given in Table I. Here, we list the energy differences calculated with three different density functionals, namely, PBE, BLYP, and B3LYP (all-electron calculation). For each size of clusters, the calculated lowest-energy isomers are highlighted with the bold-faced number **0.000** in Table I. We also performed vibrational frequency calculations for a number of clusters at B3LYP/6-31G($d$) of theory and found that the zero-point energy differences among isomers are all less than 0.08 eV. Therefore, we also highlighted in Table I (using bold-faced number) those isomers having energy difference within 0.1 eV from the lowest-energy one. Some general features can be seen in Table I. First, for

TABLE II. Calculated binding energy per atom for the lowest-energy isomer highlighted in Table I. $Si_{29}$ (si29-1a) has the highest binding energy among the clusters considered.

| | CPMD/PBE (eV) | CPMD/BLYP (eV) | B3LYP/6-31G(d) (eV) |
|---|---|---|---|
| $Si_{21}$ | 3.871 | 3.347 | 3.302 |
| $Si_{22}$ | 3.875 | 3.336 | 3.296 |
| $Si_{23}$ | 3.874 | 3.324 | 3.289 |
| $Si_{24}$ | 3.887 | 3.340 | 3.300 |
| $Si_{25}$ | 3.898 | 3.362 | 3.320 |
| $Si_{26}$ | 3.897 | 3.352 | 3.315 |
| $Si_{27}$ | 3.893 | 3.340 | 3.302 |
| $Si_{28}$ | 3.898 | 3.353 | 3.312 |
| $Si_{29}$ | 3.916 | 3.372 | 3.332 |
| $Si_{30}$ | 3.908 | 3.359 | 3.320 |

$Si_{21}$–$Si_{29}$ (except $Si_{27}$), the predicted lowest-energy clusters are all prolate in shape. Second, for $Si_{26}$–$Si_{28}$, the PBE calculation suggests that near-spherical clusters are very competitive to be the global minima, especially for $Si_{27}$. However, BLYP and B3LYP calculations suggest that the magic-cluster-assembled clusters, either prolate or Y-shaped, are very competitive for the global minima. Third, $Si_{29}$ appears to be a special cluster because the prolate isomer si29-1a is notably lower in energy than others, regardless of PBE or BLYP calculations. This is because si29-1a contains two highly stable magic clusters $Si_{10}$. As such, it is tempting to speculate that if there is a prolate-to-spherical transition at $Si_{27}$, there may be also a *reentry transition*, namely, spherical-to-prolate structural transition at $Si_{29}$ for neutral clusters. Note that for anionic cluster $Si_{29}^-$, our previous DFT calculation [at PBEPBE/6-31G(*d*) level] showed that the near-spherical cluster si29-3a is notably lower in energy than si29-1a.[49] Lastly, for $Si_{30}$, the PBE calculation indicates that the near-spherical cluster (si30-3a) is one of leading candidates for the global minimum whereas BLYP and B3LYP calculations suggest that the hypothetical Y-shaped three-arm cluster (si30-4a) is also a leading candidate.

The size range of $26 \leqslant n \leqslant 28$ deserves more discussion. As shown in Table I, isomers from all three (or four) families can be energetically highly favorable. The richness of low-lying clusters in this size range may offer additional evidence that a structural transition is likely to occur in this size range for neutral clusters. Note that for anionic clusters, two experimental groups[49,57] have observed that the photoelectron spectra become featureless at $n=27$, suggesting coexistence of a number of low-lying isomers at this size.

In Table II, we list the calculated binding energy per atom (or cohesive energy) of the lowest-energy isomer of $Si_n$ ($n=21$-30) as a function of the cluster size $n$. It shows that the binding energy per atom increases slowly as a function of $n$. Moreover, these binding energies are all greater than those [3.860 eV (PBE), 3.322 eV (BLYP), and 3.280 eV (B3LYP)] of the global-minimum $Si_{20}$ cluster reported by Rata *et al.*[20] and Zhu *et al.*[26] This trend of binding energy per atom as a function of $n$ is consistent with the trend of measured dissociation energy (for cluster larger than $Si_{25}$) by Jarrold and Honea.[58] Note that si29-1a has the highest bind energy per atom among all clusters considered, reflecting its high stability discussed above. Finally, in Table III, we also list the total-energy differences calculated based on the local-density approximation (LDA). In some early studies DFT calculations based on LDA were used to examine the relative stability of smaller-sized silicon clusters (e.g., in Ref. 17). Thus, Table III will be useful if the LDA is selected for stability analysis. We note that for $21 \leqslant n \leqslant 25$, LDA and GGA (PBE) give consistent prediction on the global minima whereas for $26 \leqslant n \leqslant 30$, LDA favors near-spherical isomers (family III).

TABLE III. The total-energy differences of a number of low-lying isomers with respect to the predicted lowest-energy isomer. All the lowest-energy clusters are highlighted using the bold-faced number **0.000**. The DFT calculations were performed based on the local-density approximation (LDA) implemented in the CPMD code(Ref. 55).

| | CPMD/LDA $\Delta E$ (eV) |
|---|---|
| si21-1a | **0.000** |
| si21-2a | 0.150 |
| si22-1a | 0.510 |
| si22-2a | **0.000** |
| si22-2 a′ | 0.191 |
| si23-1a | 0.710 |
| si23-2a | **0.000** |
| si24-1a | 0.346 |
| si24-2a | **0.000** |
| si25-1a | **0.000** |
| si25-2a | 0.287 |
| si25-3a | 0.170 |
| si25-3a′ | 0.535 |
| si26-1a | 0.684 |
| si26-2a | 0.370 |
| si26-2a′ | 0.412 |
| si26-3a | **0.000** |
| si26-4a | 1.116 |
| si27-1a | 0.879 |
| si27-3a | **0.000** |
| si27-4a | 1.447 |
| si28-1a | 0.593 |
| si28-2a | 0.392 |
| si28-3a | **0.000** |
| si28-3a′ | 0.300 |
| si28-4a | 1.636 |
| si29-1a | 0.461 |
| si29-3a | **0.000** |
| si29-4a | 1.580 |
| si30-3a | **0.000** |
| si30-3a′ | 1.364 |
| si30-4a | 1.342 |

In conclusion, we have studied structures and relative stability of four families of low-lying clusters in the size range of $Si_{21}$–$Si_{30}$. All low-lying clusters can be constructed by using certain types of generic structural motifs. The

physical basis for these "biased" constructions was derived from previous unbiased or constrained search of the global minima for medium-sized clusters by other researchers[20,32,40,41] and by us.[35–37] For some clusters, the candidate for the global minimum appears to be unique, e.g., si21-1a, si25-1a, and si29-1a, while for others, there are multiple candidates for the global minimum. For those clusters, as pointed out in Paper III (Ref. 37), determination of the true global minima requires high-level *ab initio* calculations, for example, quantum Monte Carlo calculation or coupled-cluster calculation with a large basis set. The principal objective of this work, however, is not to determine the true global-minimum structure but to seek more generic structural features as well as patterns of structural evolution for the low-lying silicon clusters in the size range of $21 \leqslant n \leqslant 30$. As mentioned in the Introduction, the low-lying clusters in the size range of $13 \leqslant n \leqslant 22$ are most likely from two families, one containing the tricapped-trigonal-prism (TTP) $Si_9$ motif while another containing the six/six $Si_6/Si_6$ motif. In contrast, in the size range of $21 \leqslant n \leqslant 30$, particularly, in the size range of $26 \leqslant n \leqslant 28$, the low-lying clusters may be from four or even more families.

## ACKNOWLEDGMENTS

We are very grateful to valuable discussions with Professor Th. Frauenheim, Professor K. A. Jackson, Professor B. C. Pan, and Professor L.-S. Wang. This work is supported by grants from the DOE (DE-FG02-04ER46164), NSF, the Nebraska Research Initiative, and by John Simon Guggenheim Foundation and the Research Computing Facility at University of Nebraska-Lincoln.

[1] D. Tomanek and M. A. Schluter, Phys. Rev. Lett. **56**, 1055 (1986); Phys. Rev. B **36**, 1208 (1987).
[2] B. C. Bolding and H. C. Andersen, Phys. Rev. B **41**, 10568 (1990).
[3] K. Raghavachari, Phase Transitions **24–26**, 61 (1990).
[4] E. Kaxiras, Phys. Rev. Lett. **64**, 551 (1990).
[5] U. Rothlisberger, W. Andreoni, and P. Giannozzi, J. Chem. Phys. **96**, 1248 (1992).
[6] B.-L. Gu, Z.-Q. Li, and J.-L. Zhu, J. Phys.: Condens. Matter **5**, 5255 (1993).
[7] I. H. Lee, K. J. Chang, and Y. H. Lee, J. Phys.: Condens. Matter **6**, 741 (1994).
[8] U. Rothlisberger, W. Andreoni, and M. Parrinello, Phys. Rev. Lett. **72**, 665 (1994).
[9] A. Bahel and M. V. Ramakrishna, Phys. Rev. B **51**, 13849 (1995); M. V. Ramakrishna and A. Bahel, Chem. Phys. **104**, 9833 (1996).
[10] J. C. Grossman and L. Mitas, Phys. Rev. Lett. **95**, 1323 (1995).
[11] M. Menon and K. R. Subbaswamy, Phys. Rev. B **51**, 17952 (1995).
[12] J. Song, S. E. Ulloa, and D. A. Drabold, Phys. Rev. B **53**, 8042 (1996).
[13] M. R. Pederson, K. Jackson, D. V. Porezag, Z. Hajnal, and Th. Frauenheim, Phys. Rev. B **54**, 2863 (1996).
[14] A. Sieck, D. Porezag, Th. Frauenheim, M. R. Pederson, and K. Jackson, Phys. Rev. A **56**, 4890 (1997).
[15] I. Vasiliev, S. Ogüt, and J. R. Chelikowsky, Phys. Rev. Lett. **78**, 4805 (1997).
[16] K.-M. Ho, A. A. Shvartsburg, B. Pan, Z.-Y. Lu, C.-Z. Wang, J. G. Wacker, J. L. Fye, and M. F. Jarrold, Nature (London) **392**, 582 (1998).
[17] B. Liu, Z.-Y. Lu, B. Pan, C.-Z. Wang, K.-M. Ho, A. A. Shvartsburg, and M. F. Jarrold, J. Chem. Phys. **109**, 9401 (1998).
[18] B. C. Pan, C. Z. Wang, D. E. Turner, and K.-M. Ho, Chem. Phys. Lett. **292**, 75 (1998).
[19] K. Jackson, M. Pederson, C.-Z. Wang, and K.-M. Ho, Phys. Rev. A **59**, 3685 (1999).
[20] I. Rata, A. A. Shvartsburg, M. Horoi, Th. Frauenheim, K. W. M. Siu, and K. A. Jackson, Phys. Rev. Lett. **85**, 546 (2000).
[21] B. X. Li and P. L. Cao, Phys. Rev. A **62**, 023201 (2000).
[22] Z.-Y. Lu, C.-Z. Wang, and K.-M. Ho, Phys. Rev. B **61**, 2329 (2001).
[23] S. N. Behera, B. K. Panda, S. Mukherjee, and P. Entel, Phase Transitions **75**, 41 (2002).
[24] Q. Sun, Q. Wang, P. Jena, S. Waterman, and Y. Kawazoe, Phys. Rev. A **67**, 063201 (2003).
[25] X. Zhu and X. C. Zeng, J. Chem. Phys. **118**, 3558 (2003).
[26] X. Zhu, X. C. Zeng, Y. Lei, and B. Pan, J. Chem. Phys. **120**, 8985 (2004).
[27] A. A. Shvartsburg, M. Horoi, and K. A. Jackson, *Spectroscopy of Emerging Materials* (Kluwer, Dordrecht, 2004).
[28] J. R. Chelikowsky, Phys. Rev. Lett. **60**, 2669 (1988).
[29] J. R. Chelikowsky and J. C. Philips, Phys. Rev. Lett. **63**, 1653 (1989).
[30] E. Kaxiras and K. Jackson, Phys. Rev. Lett. **71**, 727 (1993).
[31] A. A. Shvartsburg, M. F. Jarrold, B. Liu, Z.-Y. Lu, C.-Z. Wang, and K.-M. Ho, Phys. Rev. Lett. **81**, 4616 (1998).
[32] L. Mitas, J. C. Grossman, I. Stich, and J. Tobik, Phys. Rev. Lett. **84**, 1479 (2000).
[33] B.-X. Li, P.-L. Cao, and S.-C. Zhan, Phys. Lett. A **316**, 252 (2003).
[34] S. Yoo, X. C. Zeng, X. Zhu, and J. Bai, J. Am. Chem. Soc. **125**, 13316 (2003).
[35] S. Yoo, J. J. Zhao, J. L. Wang, and X. C. Zeng, J. Am. Chem. Soc. **126**, 13845 (2004).
[36] S. Yoo and X. C. Zeng, Angew. Chem., Int. Ed. **44**, 1491 (2005).
[37] S. Yoo and X. C. Zeng, J. Chem. Phys. **123**, 164303 (2005).
[38] A. Tekin and B. Hartke, Phys. Chem. Chem. Phys. **6**, 503 (2004).
[39] S. Goedecker, W. Hellmann, and T. Lenosky, Phys. Rev. Lett. **95**, 055501 (2005).
[40] A. Sieck, T. Frauenheim, and K. A. Jackson, Phys. Status Solidi B **240**, 537 (2003).
[41] K. A. Jackson, M. Horoi, I. Chaudhuri, T. Frauenheim, and A. A. Shvartsburg, Phys. Rev. Lett. **93**, 013401 (2004).
[42] K. A. Jackson, M. Yang, I. Chaudhuri, and T. Frauenheim, Phys. Rev. A **71**, 033205 (2005).
[43] M. F. Jarrold and V. A. Constant, Phys. Rev. Lett. **67**, 2994 (1991).
[44] M. F. Jarrold, Science **252**, 1085 (1991).
[45] M. F. Jarrold and J. E. Bower, J. Chem. Phys. **96**, 9180 (1992).
[46] K. Fuke, K. Tsukamoto, F. Misaizu, and M. Sanekata, J. Chem. Phys. **99**, 7807 (1993).
[47] R. R. Hudgins, M. Imai, M. F. Jarrold, and P. Dugourd, J. Chem. Phys. **111**, 7865 (1999).
[48] A. A. Shvartsburg, R. R. Hudgins, P. Dugourd, and M. F. Jarrold, Chem. Soc. Rev. **30**, 36 (2001).
[49] J. Bai, L.-F. Cui, J. Wang, S. Yoo, X. Li, J. Jellinek, C. Koehler, T. Frauenheim, L.-S. Wang, and X. C. Zeng, J. Phys. Chem. A **110**, 908 (2006).
[50] J. L. Elkind, J. M. Alford, F. D. Weiss, R. T. Laaksonene, and R. E. Smalley, J. Chem. Phys. **87**, 2397 (1987).
[51] Q. L. Zhang, Y. Liu, R. F. Curl, F. K. Tittel, and R. E. Smalley, J. Chem. Phys. **88**, 1670 (1988).
[52] M. F. Jarrold and J. E. Bower, J. Phys. Chem. **92**, 5702 (1988).
[53] A. D. Becke, Phys. Rev. A **38**, 3098 (1988); J. P. Perdew, Phys. Rev. B **33**, 8822 (1986).
[54] J. P. Perdew, K. Burke, and M. Ernzerhof, Phys. Rev. Lett. **77**, 3865 (1996).
[55] J. Hutter, A. Alavi, T. Deutsch, M. Bernasconi, S. Goedecker, D. Marx, M. Tuckerman, and M. Parrinello, CPMD, Version 3.7.1, MPI für Festkörperforschung, Stuttgart, 2001.
[56] M. J. Frisch, G. W. Trucks, H. B. Schlegel *et al.*, GAUSSIAN 03, Revision C.02, Gaussian, Inc., Wallingford, CT, 2004.
[57] M. A. Hoffmann, G. Wrigge, B. V. Issendorff, J. Müller, G. Ganteför, and H. Haberland, Eur. Phys. J. D **16**, 9 (2001).
[58] M. F. Jarrold and E. C. Honea, J. Phys. Chem. **95**, 9181 (1991).